Materials Research. 2013; 16(3): 655-660
DOI: 10.1590/S1516-14392013005000053

Yttria and Ceria Doped Zirconia Thin Films Grown by Pulsed Laser Deposition

***F. Saporiti*[a]*, *R. E. Juarez*[a], *F. Audebert*[a,b], *M. Boudard*[c]**

[a]*Grupo de Materiales Avanzados, Facultad de Ingeniería, Universidad de Buenos Aires, Paseo Colon 850 (C1063ACV) Ciudad de Buenos Aires, Argentina*
[b]*Consejo Nacional de Investigaciones Científicas y Técnicas – CONICET, Argentina*
[c]*Laboratoire des Matériaux et du Génie Physique, CNRS, Grenoble-INP, Minatec, 3 parvis Louis Néel BP 257, 38 016 Grenoble Cedex 1, France*

Received: November 21, 2012; Revised: February 7, 2013

The Yttria stabilized Zirconia (YSZ) is a standard electrolyte for solid oxide fuel cells (SOFCs), which are potential candidates for next generation portable and mobile power sources. YSZ electrolyte thin films having a cubic single phase allow reducing the SOFC operating temperature without diminishing the electrochemical power density. Films of 8 mol% Yttria stabilized Zirconia (8YSZ) and films with addition of 4 weight% Ceria (8YSZ + 4CeO_2) were grown by pulsed laser deposition (PLD) technique using 8YSZ and 8YSZ + 4CeO_2 targets and a Nd-YAG laser (355 nm). Films have been deposited on Soda-Calcia-Silica glass and Si(100) substrates at room temperature. The morphology and structural characteristics of the samples have been studied by means of X-ray diffraction and scanning electron microscopy. Films of a cubic-YSZ single phase with thickness in the range of 1-3 μm were grown on different substrates.

Keywords: *solid oxide fuel cells (SOFCs), Yttria-stabilized Zirconia (YSZ), pulse laser deposition (PLD), thin films*

1. Introduction

Solid oxide fuel cells (SOFCs) have been studied intensively because they exhibit a clean and efficient power generation and do not require high purity fuel. SOFCs are typically composed of two porous electrodes with a dense electrolyte of a solid oxide ceramic material[1] in between. The anode and cathode must be porous in order to allow gas transportation, whereas the electrolyte must avoid electronic charge and gas transportation across the cell. Other desired characteristics for the cell elements are chemical stability under operational conditions, high electronic conductivity for the electrodes and electrical interconnections, high ionic conductivity and almost zero electronic conductivity for the electrolyte, chemical and mechanical compatibility for all the cell components and gases, as well as low cost. Tetragonal Zirconia exhibits high toughness but its ionic conductivity is much lower than that of cubic Zirconia. Besides, it shows a degradation process in the presence of hydroxyl ions (OH–) at low temperature (lower than 400 °C), which is inconvenient in a fuel cell. The cubic Zirconia can be fully stabilized by the addition of soluble aliovalent oxides such as CaO, MgO or Y_2O_3. The doping introduces oxygen vacancies in the lattice, improving the ionic conductivity at elevated temperatures. Yttria-stabilized Zirconia (YSZ) in particular exhibits a remarkable thermal stability and degradation resistance. The ionic conductivity in a bulk material of the Yttria doped Zirconia (ZrO_2:Y_2O_3) reaches a maximum for an Yttria content in the solid solution between 8 and 12 mol% (8YSZ-12YSZ)[2].

*e-mail: cididi@fi.uba.ar

The YSZ is a standard electrolyte for SOFCs, which are potential candidates for next generation portable and mobile power sources[3-10]. Standard YSZ electrolytes operate at high temperatures (800-1000 °C) due to their ionic conductivity properties which become efficient enough only at this temperature range. However, at such high temperatures thermal and mechanical degradation of the cell materials drastically limit its lifetime. For most applications it is necessary to decrease the operation temperature without decreasing its working performance.

Decreasing the operational temperature decreases the YSZ ionic conductivity, but this can be compensated by reducing the thickness of the electrolyte, and thus reducing ohmic losses[4,6-12]. Thin and dense YSZ electrolytes can be fabricated by different techniques such as physical or chemical vapor deposition (PVD, CVD), plasma enhanced CVD (PECVD), sol-gel method, electrochemical vapor deposition, suspension or atmospheric plasma spraying[13-14], pulsed laser deposition (PLD)[15], etc. PLD allows producing films with thickness from 1 nm up to one micron scale, whereas other techniques allow producing thicker films in the range of 100 nm to 20 μm[16]. PLD is commonly used to produce thin films of a great variety of materials because the stoichiometry obtained is transferred from the target to the film. Moreover, this technique produces films with good adherence and allows growing crystalline thin films[17-18]. The thickness and structure of the film can be modified changing the deposition parameters, such as: laser wavelength, laser fluence, deposition time, substrate material, substrate temperature, etc[19-24].

It has been observed that Ce-based electrolytes have high conductivity at temperatures lower than 800 °C[25]. It is of interest to investigate the effect of CeO_2 addition to the 8YSZ produced by PLD. In this work, thin films of cubic single phase of 8YSZ + 4 wt.% CeO_2 grown on Si(100) substrate by means of PLD are presented for the first time, as far as the authors know. Also thin films of cubic single phase of 8YSZ have been produced by the same technique. The morphology, structure, thickness and porosity of the films were studied using X-ray diffraction (XRD) and scanning electron microscopy (SEM).

2. Experimental

Film samples of 8YSZ and 8YSZ + 4 wt.% CeO_2 were produced by PLD on Soda-Calcia-Silica glass and polished Si(100) substrates with different deposition times using a pulsed Nd-YAG laser. The substrates were situated at 25 mm in front of the target. Table 1 summarizes the samples' codes, compositions, substrates and processing conditions of each studied samples. The targets were prepared with the same composition of the films to be deposited. They were prepared from powders by ball milling, powder dry pressing and air sintering disk shapes of 25 mm in diameter and 1.5 mm thickness between 1450 °C and 1560 °C. The Nd-YAG laser used in this work (Spectra-Physics, Model Lab-190, USA) can be operated at 266 nm, 355 nm, 532 nm, and 1064 nm wavelengths. In this work pulses were produced at 355 nm wavelength with 8 ~ 12 ns width, an energy density of 3 $J.cm^{-2}$ per pulse and a 30 Hz repetition rate using the Q-switching operating mode. The laser beam is reflected and guided by a set of mirrors and focusing lenses yielding a maximum laser energy density to ablate the target. The beam was oriented at 15 degrees with respect to the surface of the target. The films were grown in a chamber with air atmosphere with a dynamic vacuum of 133 mbar. At a higher pressure, no films grew, only powder deposited on the substrates was observed. The chamber is mounted on a Zaber's T-series high precision PC controlled X-Y table that allows ablating a selected area on the target. The target was moved in X and Y directions having an irradiation time of 30 seconds for each position.

The morphology, microstructure and the thickness of the deposited films were analysed by secondary electron (SE) images of the surfaces and cross-sections of each sample using a Jeol 6510 LV SEM and a Philips XL30 SEM equipped with an energy dispersive X-ray (EDX) detector. The chemical compositions were checked by EDX analysis using accelerating voltages of 15 to 25 kV. Phase purity and crystallinity were studied by X-ray diffraction (XRD) in Bragg-Brentano geometry using a BRUKER D8 advanced diffractometer with monochromatic $CuK_{\alpha 1}$ radiation (λ = 0.154060 nm) and Lynx Eye one dimension detector.

3. Results and Discussion

Figure 1 shows the XRD results of 8YSZ (M1 and M2 samples) and 8YSZ + 4CeO_2 (M3 and M4 samples) films deposited on glass and Si(100) substrates. These results show that cubic-YSZ polycrystalline single phase films were grown on both types of substrates. Diffractograms of the films and the targets are similar having both materials the same phase. The inset in the Figure 1 shows a detail of the peaks corresponding to the planes (531) and (600) from both 8YSZ + 4CeO_2 targets. It is observed that the addition of CeO_2 to 8YSZ produces peak broadening and shifts toward lower angles (see Figure 1 and inset).

The unit cell parameter determined for the 8YSZ cubic-phase grown on both types of substrates (samples M1 and M2) is 0.5319 nm, which is in agreement with the unit cell value given in the standards of the International database ICDD card Ner. 00-030-1468. No contribution from tetragonal-YSZ phase was identified neither in the film (see Figure 1) nor in the target (see inset of Figure 1). No significant texture in the films were observed, which means that no preferential epitaxial growth was induced on the Si(100) substrate.

The addition of 4 wt.% CeO_2 to the 8YSZ produces peak broadening and shifts toward lower angles in the X-ray diffractogram of the samples M3 and M4 with respect to the X-ray diffractogram samples M1 and M2 in agreement with the observation in the targets (see inset Figure 1). These shifts can be explained by a Vegard law[26,27] taking into account that the substitution of Zr by Ce increases the parameters of the unit cell due to the difference in the cationic radii (r_{Ce}^{4+} = 0.97 Å and r_{Zr}^{4+} = 0.84 Å in 8-fold coordination[28]).

The classical Williams-Hall representation was used to separate the broadening of the XRD peaks induced by the crystallite size from that arising from the strains distribution. It was determined that all the films have very similar crystallite size of ~100 nm. Therefore, the largest peak broadening for the Ce doped samples respect to the un-doped Ce samples is due to the larger strains distribution (7 times larger) related to the local strain generated by the difference in the cation size between Ce^{4+} and Zr^{4+}.

Figure 2 shows EDX spectrum of the sample M2, 8YSZ film grown on Si (100). No contaminant elements were found in any of the samples, as shown in the EDX spectra. Additional peaks from the substrates were also observed.

Figure 3a, b shows SE images from cross-section of samples M3 and M4 respectively. Different layers that form the deposited films can be seen (Figure 3a). Porosity is also observed in some cross sections (see arrows in Figure 3a, b).

Table 1. Samples' codes, compositions, substrates and processing conditions.

Sample	Material	Substrate	Pressure (mbar)	Deposition time (minutes)
M1	8YSZ	Soda-Calcia-Silica glass	133	383
M2	8YSZ	Polished Si(100)	133	121
M3	8YSZ + 4CeO_2	Polished Si(100)	133	275
M4	8YSZ + 4CeO_2	Polished Si(100)	133	150

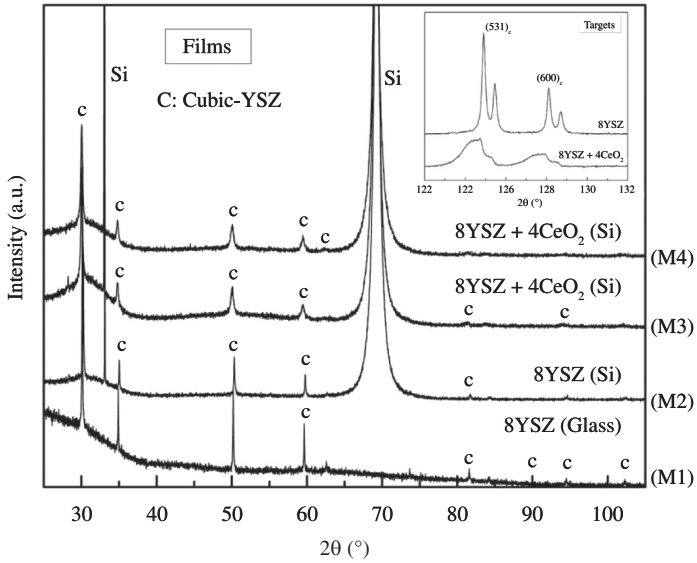

Figure 1. X-ray diffractogram of 8YSZ and 8YSZ + $4CeO_2$ films deposited on glass and Si(100) substrates, inset X-ray diffractograms of 8YSZ and 8YSZ + $4CeO_2$ targets. In particular no peaks corresponding to tetragonal phase were found in the 2θ range at 43°, 52° and 53° in the films and from 123° to 132° in the targets (see inset). C: cubic-YSZ phase.

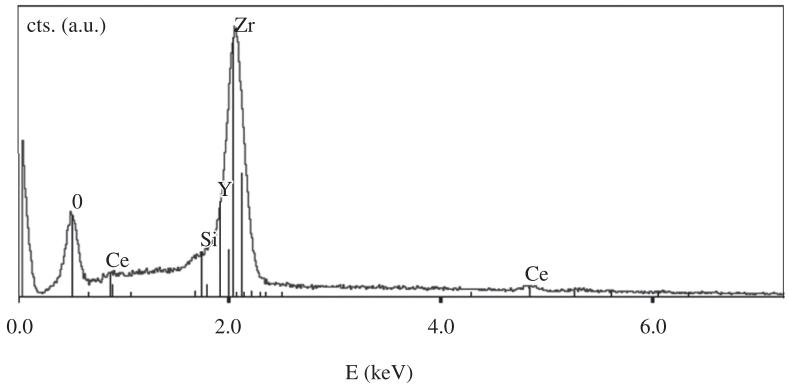

Figure 2. EDX spectrum of the sample M2. Accelerating voltage used was 15 kV.

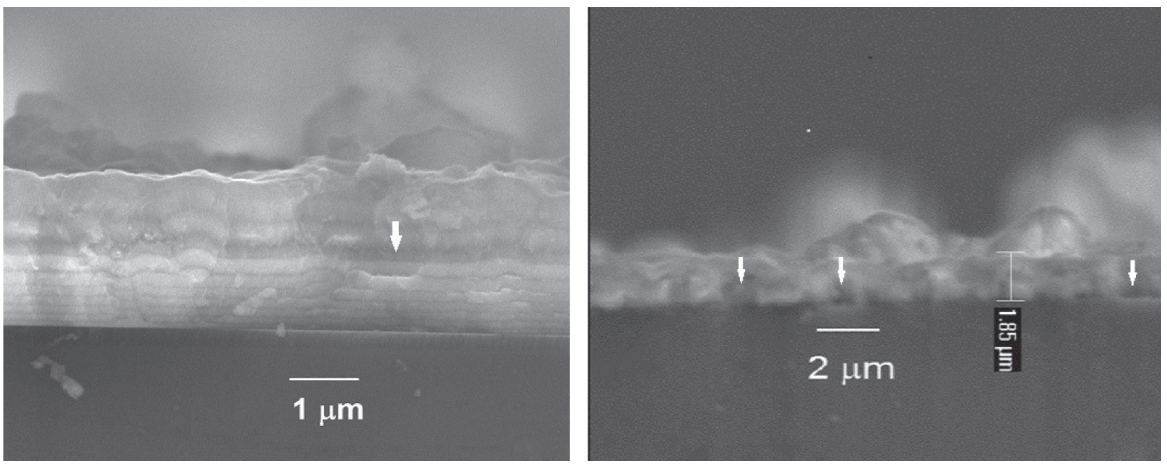

(a) (b)

Figure 3. SE images from cross-section of the samples M3 (a) and M4 (b). The arrows show the porosity in the samples.

Figure 4 shows the thickness of the film grown on Si(100) substrate at room temperature as a function of deposition time. The average value of the thickness of each film was measured on the cross section SE images, as it is shown in Figure 3b. The particulates on the film surface were not taken into account in the measurements. The error bars represent the standard deviation of thickness measured at different point along the cross section. Despite the fact that the ablation points were changed by moving the target with an interval of 30 seconds, the plume deflection effect due to the surface roughness produced by the ablation process led to slightly non-uniform thickness of the films[29]. Thicknesses obtained were between 1 to 3 μm and are correlated with deposition time. The relationship between thickness and deposition time is slightly smaller than linear regression. This phenomenon has been observed previously and it is suggested to be correlated with a reduction in the amount of target material being vaporized by the laser beam[30,31]. Krajnovich and Vazquez[32,33] have observed that the thickness-increasing trend stops with prolonged deposition time when periodic structures such as ripples, ridges, and cones are formed on the target material.

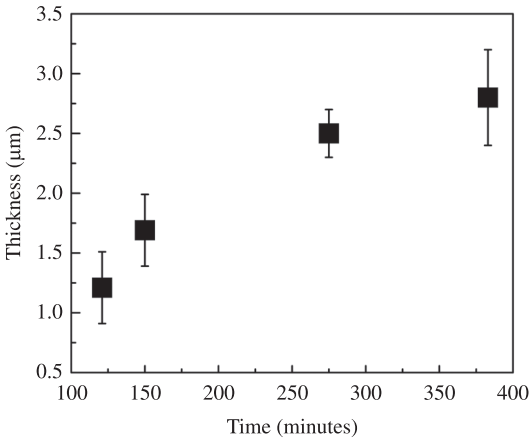

Figure 4. Thickness of the films as a function of deposition time.

Figure 5 shows SE images of the top view on the films surface of 8YSZ an 8YSZ + 4CeO_2 samples. Some micro-sized fragments or particulates as 1-5 μm spherical or quasi-spherical clusters are clearly visible on the surface of all the samples. The presence of the particulates is a characteristic of the PLD films[34]. The sample M1 has irregular particulates, which are different to the ones deposited in the other samples. The gas pressure in the chamber limits the plasma

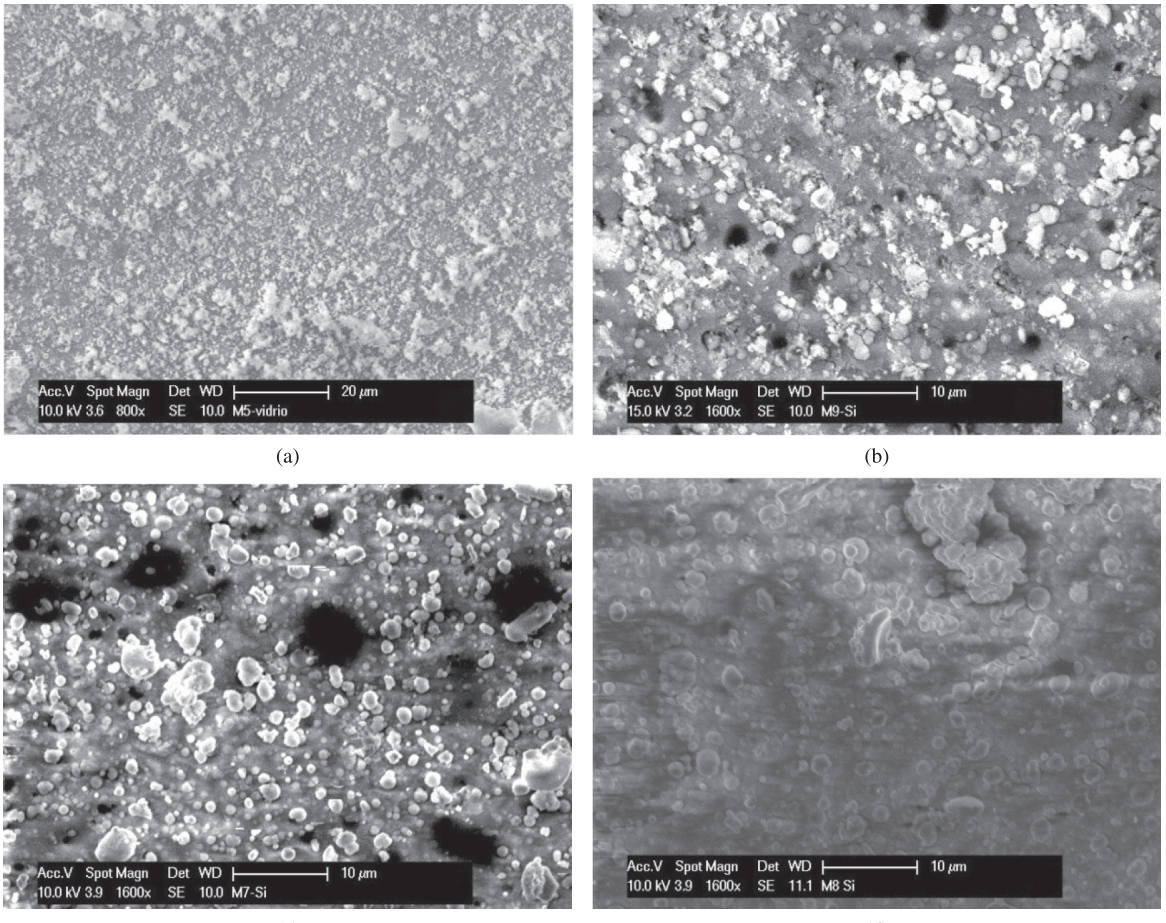

Figure 5. SE images of the surface of the samples M1 (a), M2 (b), M3 (c) and M4 (d) respectively.

plume expansion, which increases the probability of collisions between the ablated particles and thus leads to the nucleation and growth of clusters (particulates) that are deposited on the substrate during the film growth. Porosity is also observed in some of the films (M2, M3) produced on Si(100) substrate. It is expected a more compact film of Yttria and Ceria doped Zirconia cubic phase can be obtained at a lower pressure than 100 mbar.

4. Conclusion

Films of cubic phase of Yttria and Ceria doped Zirconia, 8YSZ and 8YSZ + 4 wt.% CeO_2, have been obtained by means of PLD technique using a Nd-YAG laser with 355 nm wavelength. The ablation process was produced on sintered targets at low pressure air atmosphere. The films grew without any texture and with the same cubic structure present in the targets. All the samples show crystallites of the cubic Zirconia phase with size of ~100 nm.

The cubic phase in the 8YSZ films has a unit cell parameter of 0.5319 nm. Whereas, the cubic phase in the 8YSZ + 4 wt.% CeO_2 films has larger unit cell and local strain distribution generated by the larger cation size of Ce^{4+} respect to the Zr^{4+}.

The growth rate is smaller than a linear correlation between thickness and deposition time due to a decrease in the ablated material from the target during the ablation process. All films grown on Si(100) substrates show similar surface morphology with similar particulates size.

Yttria and Ceria doped Zirconia films can be produced with cubic phase without any texture on crystalline and amorphous substrates by means of PLD technique. Further work on the films properties are required in order to evaluate the performance to the Yttria and Ceria doped Zirconia cubic phase to be used as electrolyte in solid oxide fuel cells.

Acknowledgements

This work was partially funded by the Argentine agency FONCyT (PICT-RAICES 2010 Ner. 2351) and the University of Buenos Aires (UBACYT 2010 Ner. 058). F. Audebert also thanks Erasmus Mundi FAME Program.

References

1. Sammes NM, Bove R and Pusz J. Solid Oxide Fuel Cells. In: Sammes NM. *Fuel cell techbology*. London: Edt. Springer; 2006. chap. 1, p. 1-26. http://dx.doi.org/10.1007/1-84628-207-1_1
2. Fergus JW. Electrolytes for solid oxide fuel cells. *Journal of Power Sources*. 2006; 162:30-40. http://dx.doi.org/10.1016/j.jpowsour.2006.06.062
3. Noh H, Park J, Son J, Lee H, Lee J and Lee H. Physical and Microstructural Properties of NiO- and Ni-YSZ Composite Thin Films Fabricated by Pulsed-Laser Deposition at T≤700°C. *Journal of the American Ceramic Society*. 2009; 92(12):3059-64. http://dx.doi.org/10.1111/j.1551-2916.2009.03362.x
4. Noh H, Son J, Lee H, Song H, Lee H and Lee J. Low Temperature Performance Improvement of SOFC with Thin Film Electrolyte and Electrodes Fabricated by Pulsed Laser Deposition. *Journal of the Electrochemical Society*. 2009; 156(12):B1484-B1490. http://dx.doi.org/10.1149/1.3243859
5. Kim S, Son J and Lee K. Substrate effect on the electrical properties of sputtered YSZ thin films for co-planar SOFC applications. *Journal of Electroceramics*. 2010; 24(3):153-60. http://dx.doi.org/10.1007/s10832-008-9550-y
6. Bieberle-Hutter A, Beckel D, Infortuna A, Muecke UP, Rupp JLM and Gauckler LJ. A micro-solid oxide fuel cell system as battery replacement. *Journal of Power Sources*. 2008; 177:123-30. http://dx.doi.org/10.1016/j.jpowsour.2007.10.092
7. Evans A, Bieberle-Hutter A, Rupp JLM and Gauckler LJ. Review on microfabricated micro-solid oxide fuel cell membranes. *Journal of Power Sources*. 2009; 194:119-29. http://dx.doi.org/10.1016/j.jpowsour.2009.03.048
8. Ignatiev A, Chen X, Wu N, Lu Z and Smith L. Nanostructured thin solid oxide fuel cells with high power density. *Dalton Transactions*. 2008; 40:5501-.6
9. Litzelman SJ, Hertz JL, Jung W and Tuller HL. Opportunities and Challenges in Materials Development for Thin Film Solid Oxide Fuel Cells. *Fuel Cells*. 2008; 8:294-302. http://dx.doi.org/10.1002/fuce.200800034
10. Huang H, Nakamura M, Su PC, Fasching R, Saito Y and Prinz FB. High-Performance Ultrathin Solid Oxide Fuel Cells for Low-Temperature Operation. *Journal of the Electrochemical Society*. 2007; 154(1):B20-B24. http://dx.doi.org/10.1149/1.2372592
11. Steele BCH and Heinzel A. Review article Materials for fuel-cell technologies. *Nature*. 2001; 414:345. http://dx.doi.org/10.1038/35104620
12. Will J, Mitterdorfer A, Kleinlogel C, Perednis D and Gauckler LJ. Fabrication of thin electrolytes for second-generation solid oxide fuel cells. *Solid State Ionics*. 2000; 131:79-96. http://dx.doi.org/10.1016/S0167-2738(00)00624-X
13. Beckel D, Bieberle-Hutter A, Harvey A, Infortuna A, Muecke UP, Prestat M et al. Thin films for micro solid oxide fuel cells. *Journal of Power Sources*. 2007; 173:325-45. http://dx.doi.org/10.1016/j.jpowsour.2007.04.070
14. Wincewicz KC and Cooper JS. Taxonomies of SOFC material and manufacturing alternatives. *Journal of Power Sources*. 2005; 140:280-96. http://dx.doi.org/10.1016/j.jpowsour.2004.08.032
15. Rodrigo K, Knudsen J, Pryds N, Schou J and Linderoth S. Characterization of yttria-stabilized zirconia thin films grown by pulsed laser deposition (PLD) on various substrates. *Applied Surface Science*. 2007; 254:1338-42. http://dx.doi.org/10.1016/j.apsusc.2007.07.194
16. Hidalgo H, Reguzina E, Millon E, Thomann AL, Mathias J, Boulmer-Leborgne C et al. Yttria-stabilized zirconia thin films deposited by pulsed-laser deposition and magnetron sputtering. *Surface and Coatings Technology*. 2011; 205:4495-99. http://dx.doi.org/10.1016/j.surfcoat.2011.03.077
17. Holmelund E, Thestrup B, Schou J, Larsen NB, Nielsen MM, Johnson E et al. Deposition and characterization of ITO films produced by laser ablation at 355 nm. *Applied Physics A*. 2002; 74:147-52. http://dx.doi.org/10.1007/s003390100976
18. Pryds N, Toftmann B, Schou J, Hendriksen PV and Linderoth S. Electrical and structural properties of $La_{0.8}Sr_{0.2}Mn_{0.5}Co_{0.5}O_{3\pm\delta}$ films produced by pulsed laser deposition. *Applied Surface Science*. 2005; 247(1-4):466-70. http://dx.doi.org/10.1016/j.apsusc.2005.01.168
19. Gottmann J and Kreutz EW. Pulsed laser deposition of alumina and zirconia thin films on polymers and glass as optical and protective coatings. *Surface and Coatings*

Technology. 1999; 116-119:1189-94. http://dx.doi.org/10.1016/S0257-8972(99)00191-7

20. Hobein B, Tietz F, Stover D and Kreutz EW. Pulsed laser deposition of yttria stabilized zirconia for solid oxide fuel cell applications. *Journal of Power Sources*. 2002; 105:239-42. http://dx.doi.org/10.1016/S0378-7753(01)00945-4
21. Nair BN, Suzuki T, Yashino Y, Gopalakrishnan S, Sugawara T, Nakao S-I et al. An Oriented Nanoporous Membrane Prepared by Pulsed Laser Deposition. *Advanced Materials*. 2005; 17:1136-40. http://dx.doi.org/10.1002/adma.200401294
22. Joo JH and Choi GM. Electrical conductivity of YSZ film grown by pulsed laser deposition. *Solid State Ionics*. 2006; 177:1053-57. http://dx.doi.org/10.1016/j.ssi.2006.04.008
23. Delgado JC, Sanchez F, Aguiar R, Maniette Y, Ferrater C and Varela M. ArF and KrF excimer laser deposition of yttria stabilized zirconia on Si(100). *Applied Physics Letters*. 1996; 68:1048-50. http://dx.doi.org/10.1063/1.116244
24. Li P, Caroll J and Mazumder J. Room temperature growth of biaxially aligned yttria-stabilized zirconia films on glass substrates by pulsed-laser deposition. *Journal of Physics D*: Applied Physics. 2003; 36:1605. http://dx.doi.org/10.1088/0022-3727/36/13/327
25. Dudek M and Molenda J. Ceria-yttria-based solid electrolytes for intermediate temperature solid oxide fuel cell. *Materials Science-Poland*. 2006; 24(1):45-52.
26. Vegard L. Die Konstitution der Mischkristalle und die Raumfüllung der Atome. *Zeitschrift für Physik*. 1921; 5:17-26. http://dx.doi.org/10.1007/BF01349680
27. Vegard L. X-rays in the service of research on matter. Zeitschrift für Kristallographie. 1928; 67(2):239-59.
28. Shannon RD. Revised effective ionic radii and systematic studies of interatomic distances in halides and chalcogenides. *Acta Crystallographica*. 1976; A32:751-6. http://dx.doi.org/10.1107/S0567739476001551
29. Perrone A, Zocco A, Cultrera L and Guido D. Detailed studies of the plume deflection effect during long laser irradiation of solid targets. *Applied Surface Science*. 2002; 197-198:251-6. http://dx.doi.org/10.1016/S0169-4332(02)00378-1
30. Foltyn SR, Dyer RC, Ott KC, Peterson E, Hubbard KM, Hutchinson W et al. Target modification in the excimer laser deposition of $YBa_2Cu_3O_{7-x}$ thin films. *Applied Physics Letters*. 1991; 59(5):594-6. http://dx.doi.org/10.1063/1.106386
31. Lee W-K, Wong H-Y, Chan K-Y, Yong T-K, Yap S-Sh and Tou T-Y. Effects of laser fluence on the structural properties of pulsed laser deposited ruthenium thin films. *Applied Physics A*. 2010; 100:561-8. http://dx.doi.org/10.1007/s00339-010-5875-x
32. Krajnovich DJ and Vazquez JE. Formation of ''intrinsic'' surface defects during 248 nm photoablation of polyimide. *Journal of Applied Physics*. 1993; 73(6):3001-9. http://dx.doi.org/10.1063/1.353032
33. Krajnovich DJ, Vazquez JE and Savoy RJ. Impurity-Driven Cone Formation During Laser Sputtering of Graphite. *Science*. 1993; 259(5101):1590-2. http://dx.doi.org/10.1126/science.259.5101.1590
34. Chrisey DB and Hubler GK. *Pulsed laser deposition of thin films*. New York: John Wiley; 1994.